Journal of Pharmacy and Pharmacology, 2024, **76**, 1362–1378
https://doi.org/10.1093/jpp/rgae081
Advance access publication 17 July 2024
Research Paper

JPP Journal of Pharmacy and Pharmacology

OXFORD

Network pharmacology prediction, molecular docking, and molecular dynamics simulation-based strategy to explore the potential mechanism of Huashanshen dripping pill against asthma

Xiaoyu Wang[1,‡], Yansu Ji[2,‡], Xin Jin[3,‡], Miaomiao Zhou[1], Yujie Wu[1], Yanhong Xu[1], Rui Liu[1,*], Jihong Feng[4,*]

[1]College of Pharmaceutical Engineering of Traditional Chinese Medicine, Tianjin University of Traditional Chinese Medicine, State Key Laboratory of Component-based Chinese Medicine, Tianjin University of Traditional Chinese Medicine, Haihe Laboratory of Modern Chinese Medicine, Tianjin Key Laboratory of Intelligent and Green Pharmaceuticals for Traditional Chinese Medicine, 10 Poyang Lake Road, West Zone of Tuanbo New City, Jinghai District, Tianjin 301617, China
[2]Department of Pharmacy Office, Characteristic Medical Center of Chinese People's Armed Police Force, 220 Chenglin Road, Dongli District, Tianjin 300162, China
[3]Military Medicine Section, Department of Health Services, Logistics University of Chinese People's Armed Police Force, 1 Huizhihuan Road, Dongli District, Tianjin 300309, People's Republic of China
[4]Department of Respiratory Medicine, The Second Affiliated Hospital of Tianjin University of Traditional Chinese Medicine, 69 Zengchan Road, Hebei District, Tianjin 300250, China

[‡]Xiaoyu Wang, Yansu Ji, and Xin Jin contributed equally to this work.
[*]Correspondence: College of Pharmaceutical Engineering of Traditional Chinese Medicine, Tianjin University of Traditional Chinese Medicine, State Key Laboratory of Component-based Chinese Medicine, Tianjin University of Traditional Chinese Medicine, Haihe Laboratory of Modern Chinese Medicine, Tianjin Key Laboratory of Intelligent and Green Pharmaceuticals for Traditional Chinese Medicine, 10 Poyang L ake Road, West Zone of Tuanbo New City, Jinghai District, Tianjin 301617, China. E-mail: liurui@tjutcm.edu.cn (R.L.); and Department of Respiratory Medicine, the Second Affiliated Hospital of Tianjin University of Traditional Chinese Medicine, 69 Zengchan Road, Hebei District, Tianjin 300250, China. E-mail: 493507647@qq.com (J.F.)

Abstract

Objectives: Asthma is a heterogeneous disease characterized by chronic airway inflammation. Huashanshen dripping pills (HSS) are commonly utilized for relieving asthma, relieving cough, and expelling phlegm. At present, the molecular mechanism against airway inflammation remains unclear.

Methods: In this study, network pharmacology, molecular docking technology, and molecular dynamic simulation were used to predict the therapeutic pathways of HSS for asthma. The ovalbumin-induced mouse model was used to further validate the prediction by RT-qPCR, western blot, immunofluorescence, and related methods.

Key findings: The findings indicate that HSS improves lung function and relieves lung inflammation by reducing inflammatory cell infiltration around the bronchus and reducing eosinophilic counts in bronchoalveolar lavage fluid (BALF). In addition, it lowers the levels of inflammatory cytokines and the expression levels of interleukin-4, interleukin-5, and interleukin-13 mRNA. HSS also inhibits the phosphorylation and nuclear translocation of NF-κB p65 protein.

Conclusions: All results suggested that HSS can decrease airway inflammation in asthmatic mice by inhibiting NF-κB signaling pathway. This finding will shed light on how it can be used to treat asthma.

Keywords: Huashanshen dripping pill; network pharmacology; asthma; NF-κB signaling pathway; airway inflammation

Introduction

Asthma is an obstructive lung illness caused by allergens or other causes, with clinical symptoms including wheezing, coughing, and dyspnea. The increasing morbidity and mortality have posed a threat to people's health [1]. Chronic asthma presents symptoms characterized by airway inflammation and hyperresponsiveness, along with airway remodeling [2]. Airway inflammation plays a crucial role in these characteristics, for the emergence and persistence of allergic asthma. Glucocorticoids [3], β2 receptor agonists [4], and antihistamines [5] are frequently employed in asthma management. Nevertheless, when used for longer periods, they might have side effects. Hence, finding novel and efficient therapies remains an urgent necessity.

Allergic asthma is typically characterized by eosinophilic infiltration, elevated Immunoglobulin E (IgE), and T helper type 2 (Th2) -driven inflammation [6]. Several studies have shown that allergic asthma can be treated by reducing IgE. Targeted therapy against IgE is a typical therapeutic approach [7]. In addition, interleukin-4 (IL-4), interleukin-5

Received: January 15, 2024. Editorial Acceptance: June 4, 2024

© The Author(s) 2024. Published by Oxford University Press on behalf of the Royal Pharmaceutical Society. All rights reserved. For commercial re-use, please contact reprints@oup.com for reprints and translation rights for reprints. All other permissions can be obtained through our RightsLink service via the Permissions link on the article page on our site—for further information please contact journals.permissions@oup.com.

Downloaded from https://academic.oup.com/jpp/article/76/10/1362/7716259 by guest on 25 July 2025

(IL-5), and interleukin-13 (IL-13) are some of the primary therapeutic targets for asthma that are involved in this process [8]. Nuclear factor kappa-B (NF-κB) pathway is involved in the production of multiple inflammatory cytokines including tumor necrosis factor-alpha (TNF-α), and it can recruit eosinophils resulting in allergic inflammation. Currently, an increasing number of asthma therapies are used to enhance the anti-inflammatory role by suppressing NF-κB activation [9].

Studies have provided evidence that traditional Chinese medicine may be a promising alternative and adjuvant approach to asthma therapy [10]. Huashanshen dripping pills (HSS), a traditional Chinese medicine, have been clinically associated with the treatment of respiratory diseases. It is processed from *Physochlainae Radix*, the dried roots of *Physochlaina infundibularis* Kuang, which is used to treat asthma [11]. Alkaloids, coumarin, amides, flavones, and organic acids are now the principal constituents that have been isolated and identified from *Physochlainae Radix*. Among these are the amide components *trans N*-formyl-*N*-feruloyl-putrescine and *cis N*-acetyl-*N*-feruloyl-putrescine, the coumarin components scoparone, the flavones component 3-*O*-methylquercetin, the organic acid component 4hydroxybenzoic acid, and the alkaloids anisodamine and scopolamine. Furthermore, it includes volatile oils, flavonoids, and phenolic chemicals [12-16]. By comparing the retention times of $[M + H]^+$ ions in HSS, ion fragments, and accurate mass measurements, the researchers used ultra performance liquid chromatography in conjunction with quadrupole time-of-flight mass spectrometry to characterize 11 compounds in preliminary form. Based on these comparisons and the detection of blood components, the preliminary findings indicate that anisodamine is the primary active component of HSS [11]. Studies have shown that anisodamine could improve asthma with eosinophilic inflammation by regulating the balance of T helper type 1 (Th1) and Th2 [17]. Isoquercitin could suppress the eosinophilic inflammation [18]. Umbelliferone attenuated the alteration characteristics of allergic airway inflammation [19]. Since 3-*O*-methylquercetin has anti-inflammatory properties, it may be used to treat asthma [20]. 6,7-Dimethoxycoumarin could treat lipopolysaccharide (LPS)-induced immune responses via the inhibition of TLR-4/NF-κB signaling activation [21]. Recent research has reported that HSS has anti-asthma effects [22], but the molecular mechanisms that lead to the resolution of inflammation of asthma by HSS are still unknown.

In this study, network pharmacology, molecular docking methods, and molecular dynamics simulation were used to explore the underlying mechanism. Whole body plethysmograph (WBP), hematoxylin-eosin staining (H&E), immunofluorescence, enzyme-linked immunosorbent assay, real-time quantitative polymerase chain reaction (qRT-PCR), and western blot (WB) were used to verify the effect of HSS on OVA-induced asthma inflammation in mice, and to determine a mechanism of action. Thus, this research can identify the possible anti-inflammatory mechanisms of HSS, while also providing a research basis for therapeutic applications.

Materials and methods

Reagents

HSS was acquired from Zhongxin Pharmaceuticals (Tianjin, China, batch number: 640003). Injection of dexamethasone (DEX) was obtained from Jinyao Pharmaceuticals (Tianjin, China). Ovalbumin (OVA) was supplied by Sigma–Aldrich Co. (St. Louis, MO, USA). Researchers obtained the ELISA kits for IL-13, TNF-α, and OVA-specific IgE from Sino Best Biological Technology Co., Ltd (Shanghai, China). The IgE ELISA kit came from Meimian industrial Co.,Ltd (Jiangsu, China). The following antibodies were used: NF-κB p65, p-NF-κB p65 were obtained from ABclonal Technology (Wuhan, China), β-actin was picked up from Sangon Biotech (Shanghai, China). TransGen Biotech (Beijing, China) provided the PerfectStart Green Supermix and TransScript All-in-One First-Strand cDNA Synthesis Supermix.

Animals

Female BALB/c mice free of specific pathogens (n = 60, 6–8 weeks, 18–20 g) were purchased from SPF (Beijing) Biotechnology Co., Ltd (license number SCXK2019-0010, Beijing, China) and maintained in specific-pathogen-free condition. The mice were kept in an environment that was under control (a regular 12 h light/dark cycle, temperature 24 ± 1°C, and humidity of 55 ± 5%) and utilized after 7 days of acclimatization. The Tianjin University of Traditional Chinese Medicine's ethics committee gave its approval to this research (approval number TCM-LAEC2023012; dated 28 February 2023). All animal testing was done under Tianjin University of Traditional Chinese Medicine animal guidelines and the People's Republic of China Animal Protection Law.

Network pharmacology analysis

The phytochemical profile of HSS was inferred by literature search in CNKI and PubMed database, and the potential active compounds were screened from the Traditional Chinese Medicine Systems Pharmacology (TCMSP, https://old.tcmsp-e.com/tcmsp.php) database [23] as well as Swiss ADME (http://www.swissadme.ch/) platform [24]. Swiss Target Prediction tool [25] (http://www.swisstargetprediction.ch/) predicted the potential targets of the active ingredients. GeneCards (http://www.genecards.org)databases) [26], (DisGenet (https://www.disgenet.org)databases) [27], along with OMIM (https://www.omim.org) databases [28] were used to find the targets for asthma. Protein–protein interaction (PPI) was evaluated in the STRING (https://www.string-db.org) database [29] with medium confidence (0.400) after we mapped the composition targets into the asthma targets. Metascape (https://metascape.org) database [30] was used to do the biological process (BP) and Kyoto Encyclopedia of Genes and Genomes (KEGG) pathway enrichment analysis, and the free Bioinformatics online tool was used to create a bubble chart. Cytoscape 3.9.1[31] software was used to establish the "component-target-disease" network, calculate the degree centrality (DC), betweenness centrality (BC) and proximity centrality (CC) of the network graph, analyze and visualize the network topology of the interaction relationship, and evaluate the importance of the active components of HSS and their corresponding targets.

Molecular docking study

The two-dimension structures of potential active compounds in HSS were downloaded from the PubChem database (https://pubchem.ncbi.nlm.nih.gov/), and the three-dimension structures of the target protein were obtained from the PDB database (https://pubchem.ncbi.nlm.nih.gov/). AutoDock Tools 1.5.6 software was utilized to perform molecular docking analysis.

Downloaded from https://academic.oup.com/jpp/article/76/10/1362/7716259 by guest on 25 July 2025

Molecular dynamics simulation

Additionally, 100 ns molecular dynamic simulations (MD) were conducted to examine the dynamic properties of the 1IKN-anisodamine, 1NFI-3-*O*-methylquercetin, 4KIK-3-*O*-methylquercetin complexes. The MD was performed using Gromacs 2022.3 [32, 33]. The topology file was generated in Gromacs by importing the structure files of proteins and small molecules. The simulation system was then placed in the TIP3P water box model. To maintain electrical neutrality, Na^+ or Cl^- were randomly added to the simulation system. Energy minimization was performed using the steepest descent method in all simulations. MD were conducted for 100 ns at a constant temperature of 300 K and a constant pressure of 1 atm using the Amber99sb-ildn force field. The resulting data was used to calculate the root mean square variance (RMSD), root mean square fluctuation (RMSF), protein gyration radius (Rg), and hydrogen bond number.

Experimental protocol

A modified version of the method used by Kearley *et al*. was used to conduct the experiment [22]. Fig. 1 depicts the development of an allergic asthma mouse model and its treatment with HSS or DEX. At days 0 and 12, 150 µl of an intraperitoneal (i.p.) allergen injection containing 10 µg OVA and 2 mg Inject Alum was administered to the mice. Mice were exposed to 100 µg of OVA by nasal inhalation (i.n.) once daily for three days starting on day 18. The treatment with HSS [108/216/432 mg/kg intragastrical administration (i.g.)] once a day starting from Days 0 to 20. Dexamethasone (2 mg/kg i.p. once a day), as a positive drug, was dissolved in saline and administrated from Days 15 to 20. Instead, the control and model groups were given saline injections. Mice were euthanized 24 h following the final OVA test.

Lung function testing

Lung function is an important indicator of respiratory disease lesions. WBP is commonly used to measure lung function with a non-invasive approach [34]. Briefly, the measurement of lung function in mice was performed using EMKA WBP pulmonary system after the last OVA challenge and the signal streaming is collected by iox2 (version 2.9.4.32).

Collection of BALF and cell counting

PBS was given into the left lung three times, and BALF was gathered. BALF was centrifuged. The supernatant was collected and kept at −80°C, and the cell precipitate was used for counting. The total cells were counted using a hematocrit plate, and the eosinophils were counted after Wright-Giemsa staining.

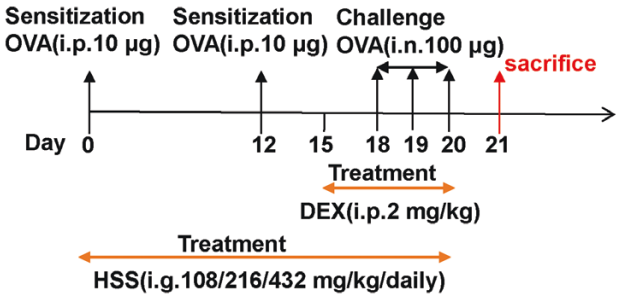


Figure 1. Experimental protocol for asthma model of allergic airway inflammation and intervention with HSS or DEX. OVA, ovalbumin; DEX, dexamethasone; HSS, Huashanshen dripping pill; i.n., nasal inhalation; i.p., intraperitoneally; i.g., intragastrical administration.

Lung histopathology analysis

The right upper lung lobe was collected and processed for histological examination. H&E staining was performed to observe the lesions [35].

ELISA assay

TNF-α and IL-13 levels were measured using ELISA assays in serum and BALF. Additionally, the amounts of serum total and OVA-specific IgE were measured. Experimental technique followed the manufacturer's instructions exactly.

qRT-PCR

Total RNA was isolated from lung tissue. The concentration was quantified, and reverse transcription was used to create cDNA from 1 µg of total RNA. The cDNA was then amplified by real-time PCR using a QuantStudio® 5 real-time PCR equipment and a reaction kit including 2 × TransStart® Tip Green qPCR SuperMix and 10 µM primers. The reaction process consisted of 40 cycles of 94°C for 5 s and 60°C for 30 s. All primers were manufactured by Sangon Biotech (Shanghai, China). In Table 1, primer sequences are displayed.

Immunofluorescence

Sections of lung tissue with paraffin (5 µm thickness) were repaired under microwave heating, blocked in goat serum (Solarbio) for 50 min, and incubated with NF-κB p65 antibody (1:100) for a whole night at 4°C. Then, the slices were incubated with the secondary antibody (1:200; Proteintech) at 25°C for 2 h. Samples were sealed by antifading mounting medium with DAPI (Solarbio) and observed under a fluorescence microscope (Leica).

Western blot

The RIPA Lysis Buffer (Beyotime) supplemented with 1% PMSF and 2% phosphatase inhibitors was used to lyse the cryopreserved lung tissues. The lung tissue lysates underwent a 15-min centrifugation at 12 000 rpm at 4°C. Thereafter, the supernatants were obtained as the total protein extracts. They were boiled for 5 min before western blot analysis as described previously. Primary antibodies included anti-NF-κB p65 and anti-p-NF-κB p65. The Wayne Rasband National Institutes of Health in the United States used Image J 1.52a to measure the intensity of the bands. Internal control was provided by β-actin.

Statistical analysis

The analysis of the data was done with GraphPad Prism 8.0. To compare the groups, one-way analysis of variance (ANOVA) was employed. The data was shown as the mean and standard deviation (mean ± SD). $P < 0.05$ was used to determine statistical significance.

Results

Exploration of potential mechanisms of HSS against asthma

In the TCMSP database, OB represents oral bioavailability and DL represents drug-likeness. A certain value is set to screen compounds with higher oral bioavailability and drug sample characteristics. The screened compounds are more likely to have good biological activity and pharmacological

Downloaded from https://academic.oup.com/jpp/article/76/10/1362/7716259 by guest on 25 July 2025

Table 1. Primer sequences of the genes for quantitative real-time polymerase chain reaction.

Target	Sequences (5′-3′)	
	Forward	Reverse
IL-4	TACCAGGAGCCATATCCACGGATG	TGTGGTGTTCTTCGTTGCTGTGAG
IL-5	CTCTGTTGACAAGCAATGAGAC	GTCTAGCCCCTGAAAGATTTCT
IL-13	CTCTTGCTTGCCTTGGTGGTCTC	GGGAGTCTGGTCTTGTGTGATGTTG
GAPDH	TGGTGAAGGTCGGTGTGAACGG	ACTGTGCCGTTGAATTTGCCCG

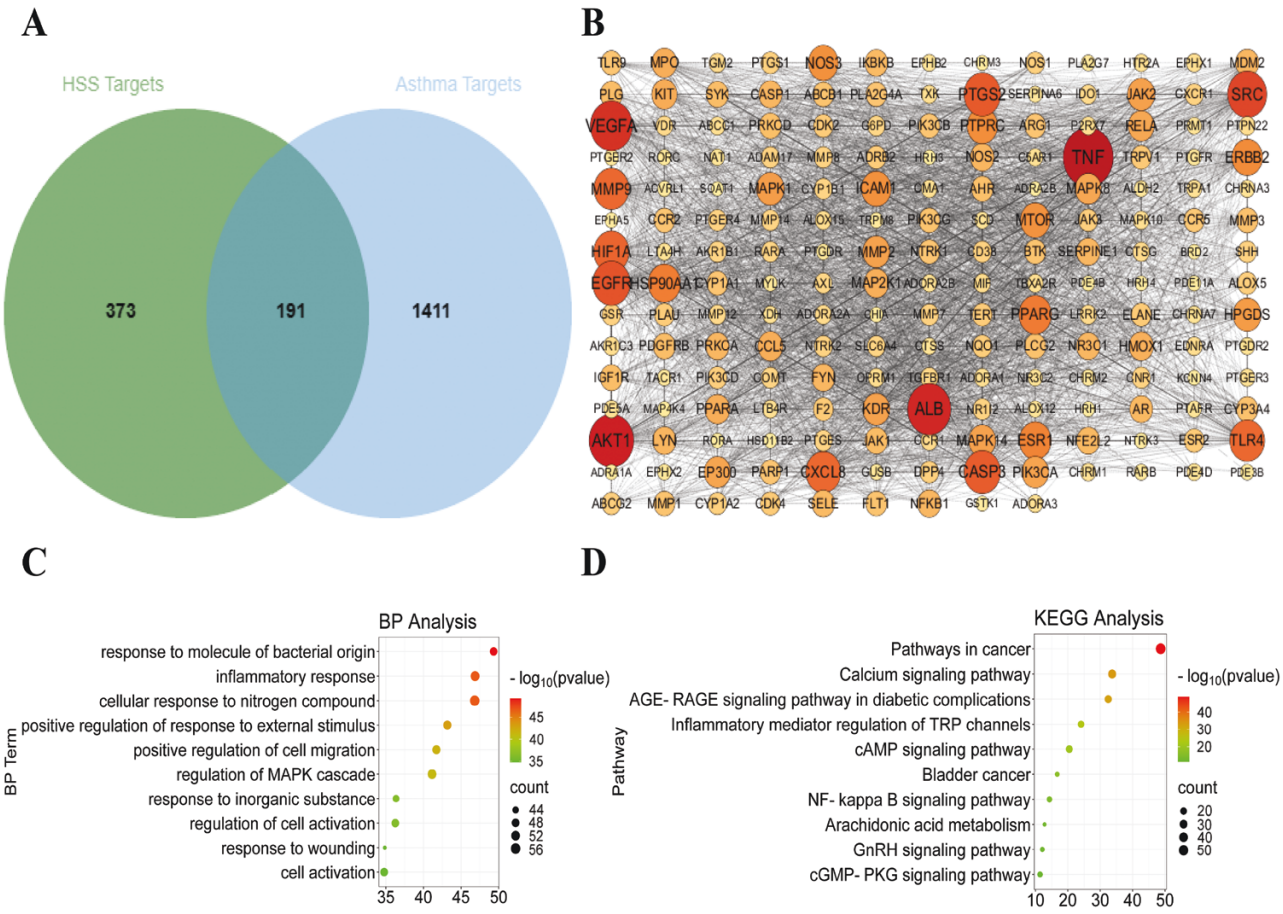


Figure 2. Analysis of potential mechanisms of HSS against asthma by network pharmacology analysis. (A) Venn Diagram revealed the shared targets between the composition targets and asthma targets. (B) PPI network of the shared targets. (C) Dot bubble of biological process analysis of the shared targets. (D) Dot bubble of KEGG pathway enrichment analysis of the shared targets.

properties. Therefore, compounds with OB ≥ 30% and DL ≥ 0.18 were screened, and compounds were screened with GI absorption shown as "High" and at least 2 parameters of Drug-likeness shown as "Yes" in Swiss ADME platform. There were 43 compounds screened as potential active ingredients and 564 targets contained in HSS. A total of 1602 asthma targets were identified through filters, with DisGeNET score ≥ 0.03 and GeneCards score ≥ 1.95. There were 191 shared targets between the drug and the disease (Fig. 2A). PPI results showed that the potential targets of HSS against asthma include TNF-α, NF-κB p65, IκB-α, Akt1, VEGFA, etc. (Fig. 2B). Targets (191) of HSS for treating asthma are mainly involved in BP such as inflammatory response, regulation of cell migration and MAPK cascade, etc (Fig. 2C). According to the findings of the KEGG enrichment study, HSS may treat asthma by influencing the NF-κB signaling pathway, the calcium signaling route, the cAMP signaling system, and other signaling pathways (Fig. 2D).

For nodes in the network, the larger the degree value of a node, the higher the importance in the network, and then combined with the BC and CC values of the network component nodes to jointly judge the importance of nodes. By constructing the " component-target-disease" network diagram (Fig. 3), components with degree values greater than 20 (2 times the median) were defined as core components, therefore 14 most likely active ingredients were further screened, as shown in Table 2.

Downloaded from https://academic.oup.com/jpp/article/76/10/1362/7716259 by guest on 25 July 2025

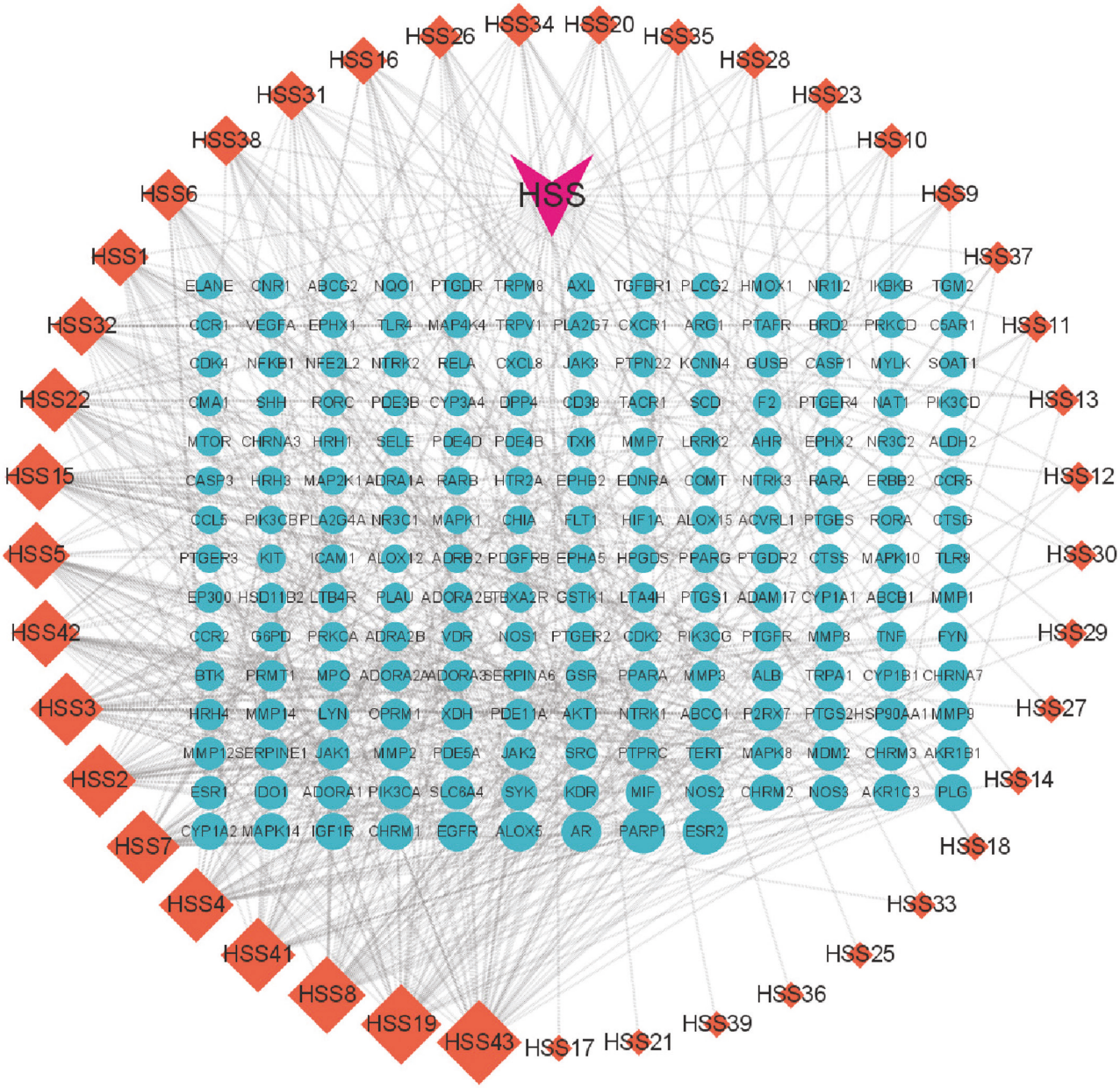


Figure 3. Network diagram of drug-ingredient-target. *Note*: The purplish red V-shaped node indicates *Physochlaina infundibularis* Kuang; the orange diamond nodes represent the active ingredients of *Physochlaina infundibularis* Kuang. The blue circular nodes represent the corresponding targets of each active ingredient.

Experimental results of molecular docking

The network pharmacology approach was employed to screen 14 active ingredients (Table 2) and 4 targets (Table 3), and the corresponding molecular docking binding energy results are presented in Table 4. In general, researchers will tend to select molecular pairs with higher binding energies for study and optimization [36] Subsequently, the top four binding energies from the docking results were selected for visual analysis using Pymol 2.2.0, the parameters of its docking process are shown in Table 5. Anisodamine binds to 1IKN by forming three hydrogen bonds with GLY183 (3.79A),THR256 (3.54A), and TYR181 (6.09A) (Figs. 4a and 5A). There are four hydrogen bonds, GLN212(3.03A), THR179 (3.30A), TYR248 (5.69A), andTHR259 (4.72A) between 3-*O*-methylquercetin and 1NFI (Figs. 4B and 5B). Similarly, there are four hydrogen bonds, THR396 (4.47A), SER613 (4.87A), ARG606 (4.60A), and THR610 (3.82A) between 3-*O*-methylquercetin and 4KIK (Figs. 4C and 5C), 3-*O*-methylquercetin binds to 5UUI by forming four hydrogen bonds with SER81 (4.35A), GLU135 (4.00A), and THR79 (3.94A, 3.50A) (Figs. 4D and 5D). In addition, there are attractions and hydrophobic interactions between molecules, such as Pi-cation, alkyl, and Pi-alkyl. Notably, these active ingredients exhibited significant affinity towards key targets within the NF-κB pathway, suggesting a potential role of HSS in asthma treatment.

Experimental results of molecular dynamics simulation

As shown in Fig. 6A, the RMSD curve (red line) of anisodamine stabilized at around 0.16 nm between 48 and 100 ns.

Downloaded from https://academic.oup.com/jpp/article/76/10/1362/7716259 by guest on 25 July 2025

Table 2. Ingredients in *Physochlaina infundibularis* Kuang with degree value > 20.

ID	Ingredient	DC	BC	CC
HSS43	Scopolamine	42	7759.39	0.41
HSS19	Tridecanoic acid	39	6884.59	0.4
HSS8	3-*O*-methylquercetin	37	6407.26	0.4
HSS41	Atropine	35	3416.51	0.4
HSS4	Hyoscyamine	35	3416.51	0.4
HSS7	6,7-Dimethoxycoumarin	34	5457.16	0.39
HSS3	*Trans N*-acetyl-*N*-feruloyl-putrescine	34	3842.05	0.39
HSS2	*Cis N*-acetyl-*N*-feruloyl-putrescine	34	3842.05	0.39
HSS5	Anisodamine	30	2552.05	0.39
HSS42	Raceanisodamine	30	2552.05	0.39
HSS15	Palmitic acid	30	3900.29	0.39
HSS22	3-Methoxy-4-propoxybenzaldehyde	28	4746.65	0.39
HSS32	Hexahydrofarnesol	24	4860.14	0.38
HSS1	*Trans N*-formyl-*N*-feruloyl-putrescine	23	1907.51	0.38

Table 3. Molecular docking receptor information.

Target protein	Gene name	PDB ID
NF-kappa-B inhibitor alpha	NFKBIA	1IKN
Transcription factor p65	RELA	1NFI
Inhibitor of nuclear factor kappa-B kinase subunit beta	IKBKB	4KIK
Tumor Necrosis Factor	TNF	5UUI

Table 4. Binding energy results of molecular docking (kcal/mol).

ID Target	1IKN	1NFI	4KIK	5UUI
HSS7	−6	−5.5	−6.9	−6.5
HSS19	−4.4	−4.4	−4.6	−4.4
HSS4	−7	−6.2	−7.1	−5.9
HSS41	−5.5	−6.2	−7.2	−5.8
HSS43	−5.6	−6.3	−7.7	−6.3
HSS8	−7	−7.1	−8.5	−6.9
HSS32	−5.5	−4.9	−5	−4.8
HSS5	−7.2	−6.8	−7.1	−5.9
HSS42	−5.6	−6.3	−7.7	−6
HSS15	−5.1	−4.4	−5.1	−4.3
HSS22	−5.2	−5.1	−5.9	−5.4
HSS1	−6.2	−5.4	−6.4	−5.1
HSS3	−5.1	−5.2	−7.2	−5.7
HSS2	−5.8	−5.6	−6.8	−6.1

Similarly, the RMSD curve of 1IKN(blue line) was stable at 0.58–0.64 nm for 60–100 ns. The RMSD curve of 1IKN-anisodamine complex (green line) was also stable around 0.60–0.66 nm for 60 to 100 ns. These results indicate that anisodamine and 1IKN could form a stable complex system. Fig. 6B illustrates that residues 60–80, 280–300, and 300–340 of 1IKN exhibited greater residue flexibility. Fuethemore,

Table 5. Parameter information for docking.

PDB ID	The central coordinates (x,y,z)	Grid box (x,y,x)
1IKN	30.467, 25.164, 12.395	52 28 50
1NFI	−0.368, 67.655, 73.168	72 76 126
4KIK	25.754, −2.582, −85.608	96 54 92
5UUI	45.301, 52.93, 13.768	28 40 44

Fig. 6C shows that the Rg values of 1IKN remained stable between 70 and 100 ns, with the lowest average Rg values between 2.96 and 3.00 nm. Finally, the 1IKN-Anisodamine complex had a maximum of four hydrogen bonds (Fig. 6D).

Fig. 7A displays that the RMSD curve (red line) of 3-*O*-methylquercetin remained stable around 0.10 nm from 28 to 100 ns. The RMSD curve of 1NFI (blue line) was also found to be stable at 0.60–0.70nm for 68–90 nm. The RMSD of 1NFI-3-*O*-methylquercetin complex (green line) was determined to stay stable around 0.60–0.80nm for 68–90 ns, indicating that 1NFI and 3-*O*-methylquercetin could form a settled complex system. 1NFI has greater residue flexibility at residues 70–80, 250–260, and 330–340 (Fig. 7B). Fig. 7C depicts that the Rg values of 1NFI remained stable between 6 and 90 ns, with the lowest average Rg values between 3.08 and 3.15 nm. The maximum number of hydrogen bonds in the 1NFI-3-*O*-methylquercetin complex was 7 (Fig. 7D).

In Fig. 8B, the RMSD curve of 4KIK (blue line) was stable at 0.70–0.90 nm for 30–60 ns, while the RMSD of its complex (green line) stabilized around 0.90–1.00nm at 30–60 ns, indicating that 4KIK and 3-*O*-methylquercetin could form a robust complex system. The Rg values of 4KIK remained stable between 40 and 60 ns, with the lowest average Rg values between 5.00 and 5.10 nm (Fig. 8C). And the complex had at most four hydrogen bonds (Fig. 8D).

MD revealed that anisodamine and 1IKN, as well as 3-*O*-methylquercetin and 1NFI, 4KIK could form stable complexes. However, the molecules of 3-*O*-methylquercetin and 5UUI separated from the protein at 62 ns, indicating that they were unable to form stable complexes.

HSS improved the lung functions of asthmatic mice

Non-invasive animal lung function detection system was used to assess enhanced pause (Penh), respiratory rate (F), and tidal volume (TV), which are used as indicators of airway resistance [37,38]. As seen in Fig. 9, Penh of OVA-induced asthma model mice was dramatically extended, F rose ($P <$ .01), and TV decreased compared to mice in the blank group. The F of mice in the DEX group was dramatically reduced ($P < 0.01$) and the Penh of mice in the high-dose group and DEX group declined significantly ($P < 0.01$) when compared to the model group. HSS tented to improve the respiratory rate and tidal volume disorder of asthmatic mice, nevertheless, there was no statistically significant change ($P > 0.05$). The results showed that HSS could improve lung dysfunction in OVA-induced asthmatic mice.

HSS diminished inflammatory cells recruitment in BALF

OVA exposure causes an increase in inflammatory cells in the lungs of mice, and eosinophils among these cells play a significant role in the development of allergen-induced asthma.

Downloaded from https://academic.oup.com/jpp/article/76/10/1362/7716259 by guest on 25 July 2025

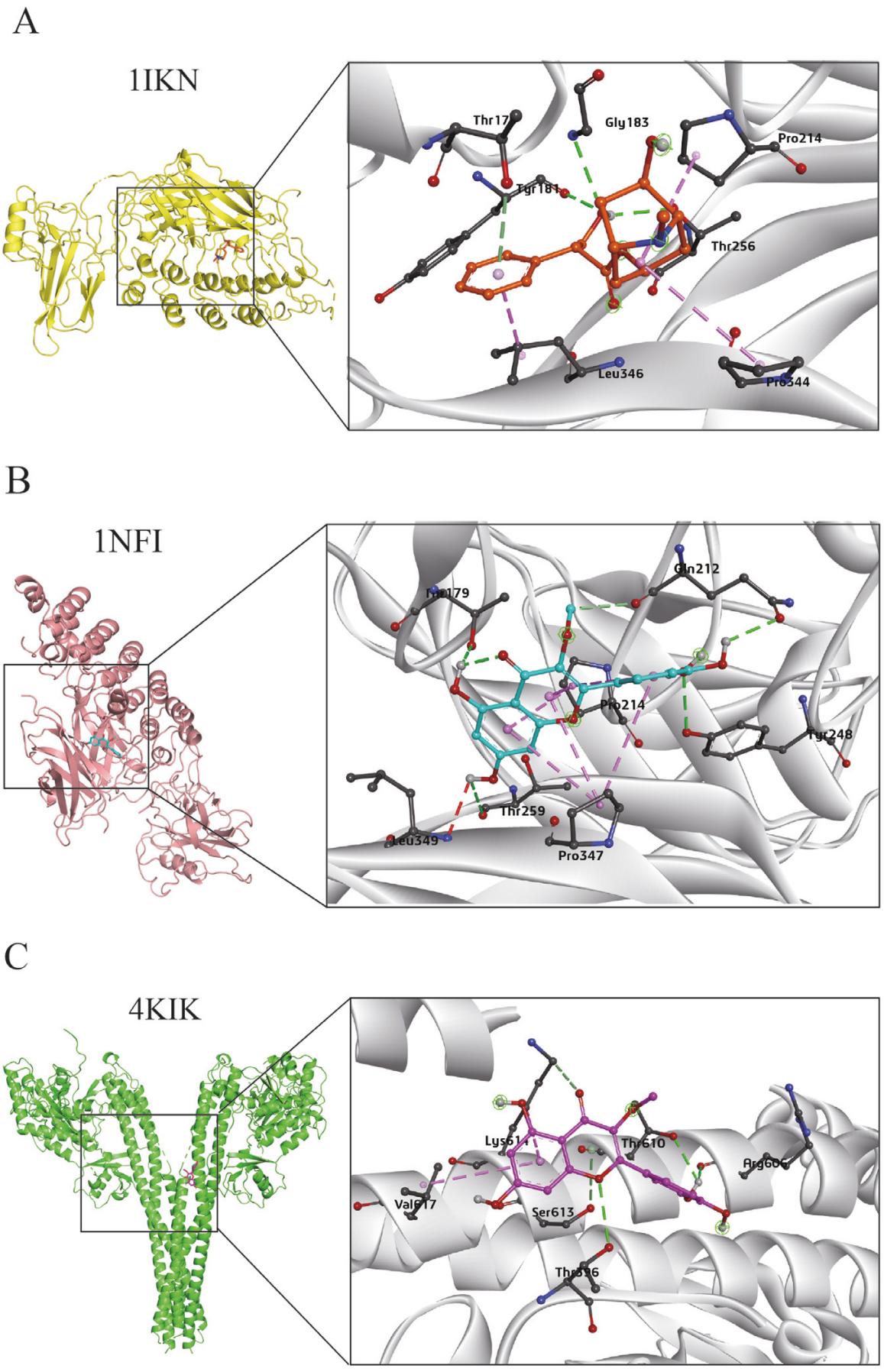


Figure 4. Molecular docking diagram. A: Docking results of anisodamine and 1IKN; B: docking results of 3-*O*-methylquercetin and 1NFI; C: docking results of 3-*O*-methylquercetin and 4KIK; D: docking results of 3-*O*-methylquercetin and 5UUI.

Downloaded from https://academic.oup.com/jpp/article/76/10/1362/7716259 by guest on 25 July 2025

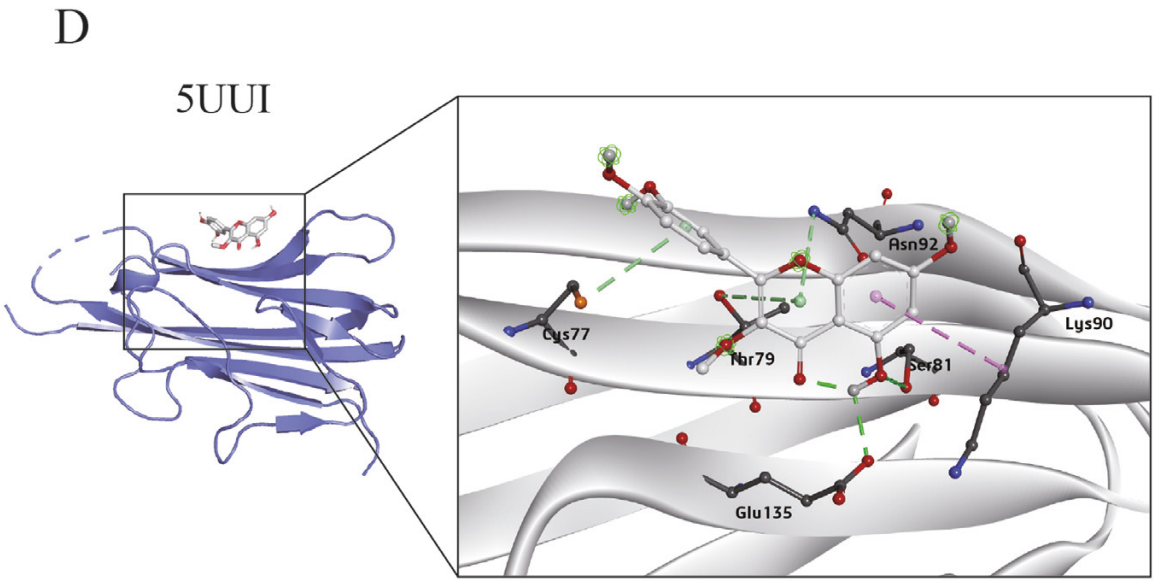


Figure 4. Continued

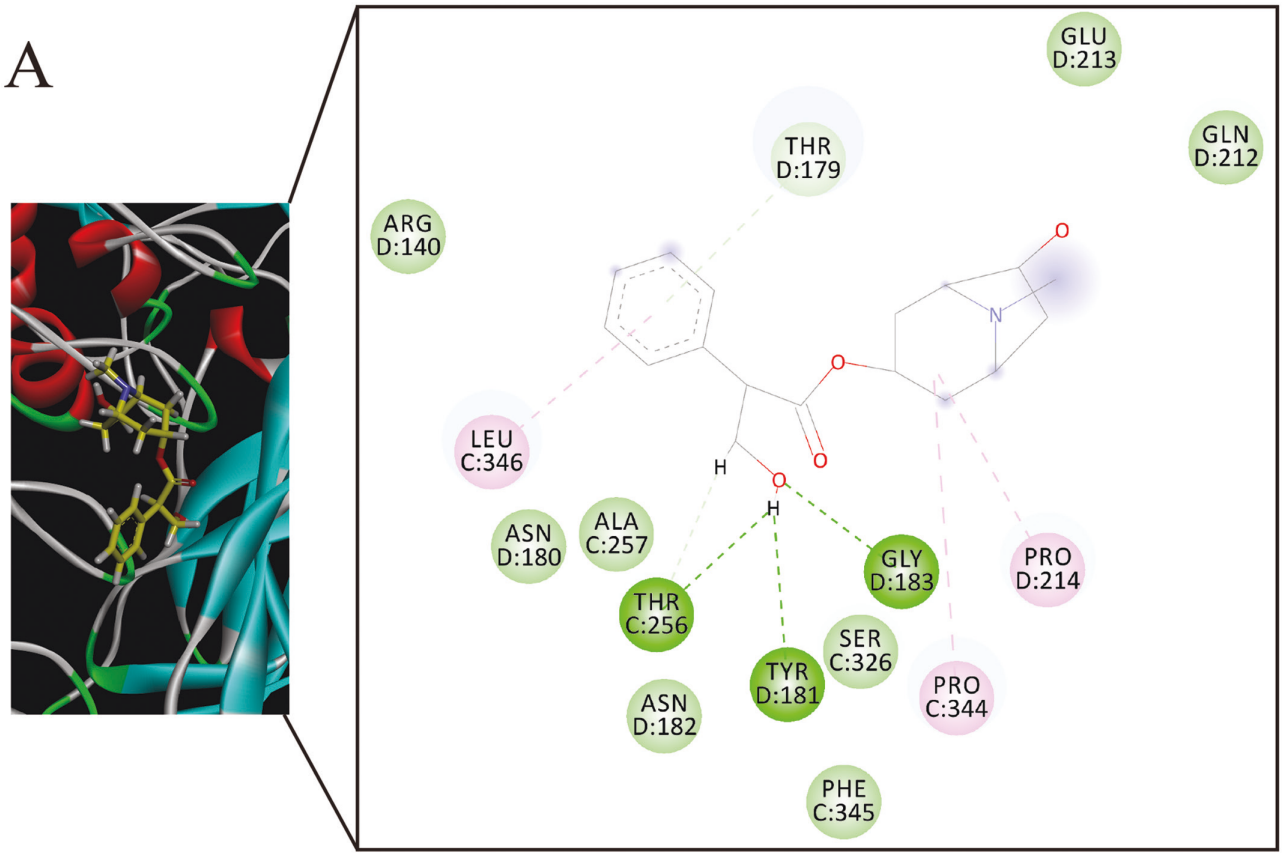


Figure 5. Molecular docking two-dimensional ligand interaction diagram. A: Docking results of anisodamine and 1IKN; B: docking results of 3-*O*-methylquercetin and 1NFI; C: docking results of 3-*O*-methylquercetin and 4KIK; D: docking results of 3-*O*-methylquercetin and 5UUI.

To analyze the role of HSS on the inflammatory response, the total number of cells and eosinophils were counted from BALF. In contrast to the control group, the results displayed that total leukocytes and eosinophils were significantly increased in the mice after OVA exposure ($P < 0.01$) (Fig. 10A and B). HSS (432 mg/kg) drastically reduced the total leucocyte numbers ($P < 0.05$) (Fig. 10A). In addition, HSS decreased the eosinophils in different doses (Fig. 10B).

Downloaded from https://academic.oup.com/jpp/article/76/10/1362/7716259 by guest on 25 July 2025

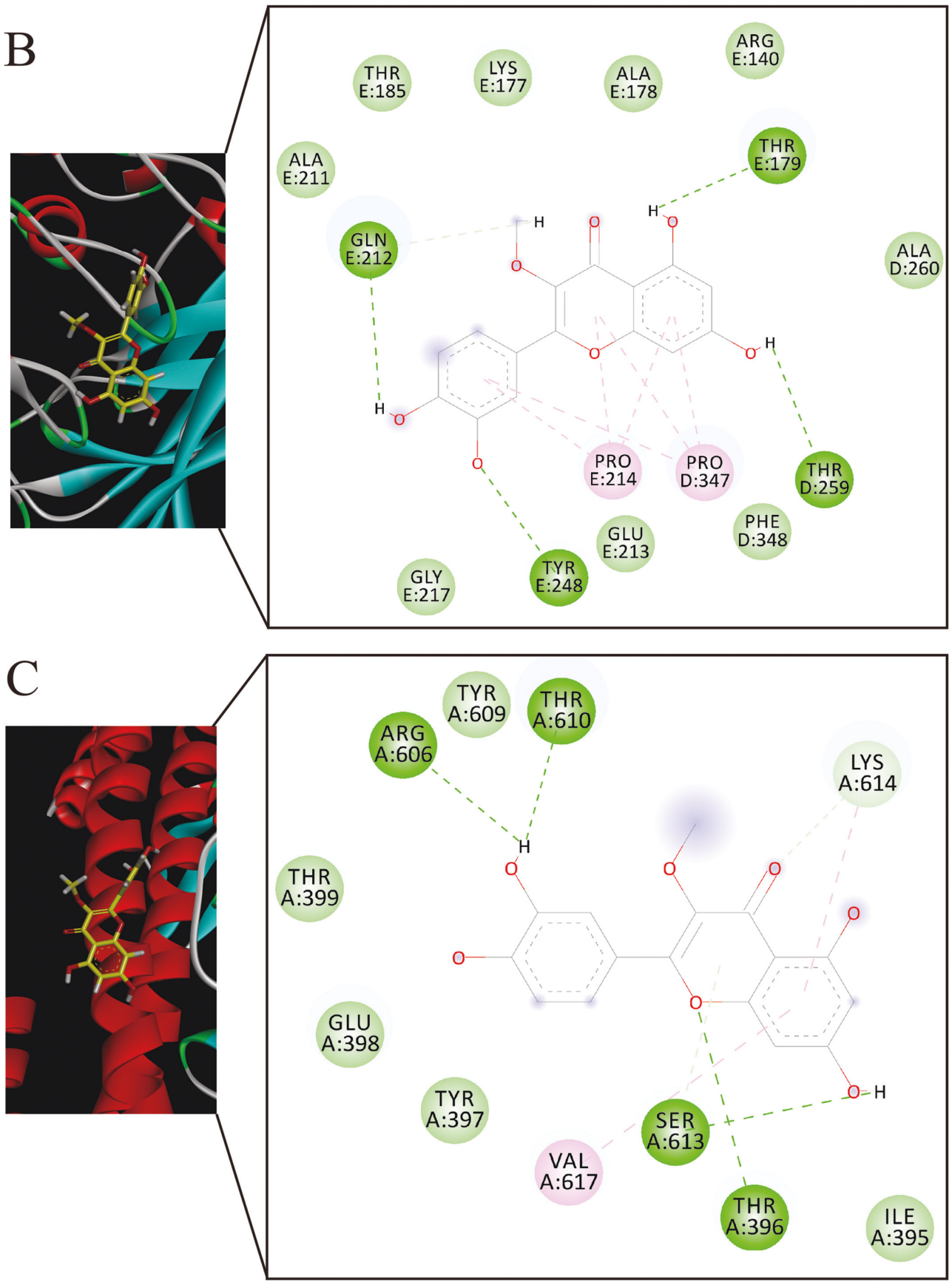


Figure 5. Continued

Downloaded from https://academic.oup.com/jpp/article/76/10/1362/7716259 by guest on 25 July 2025

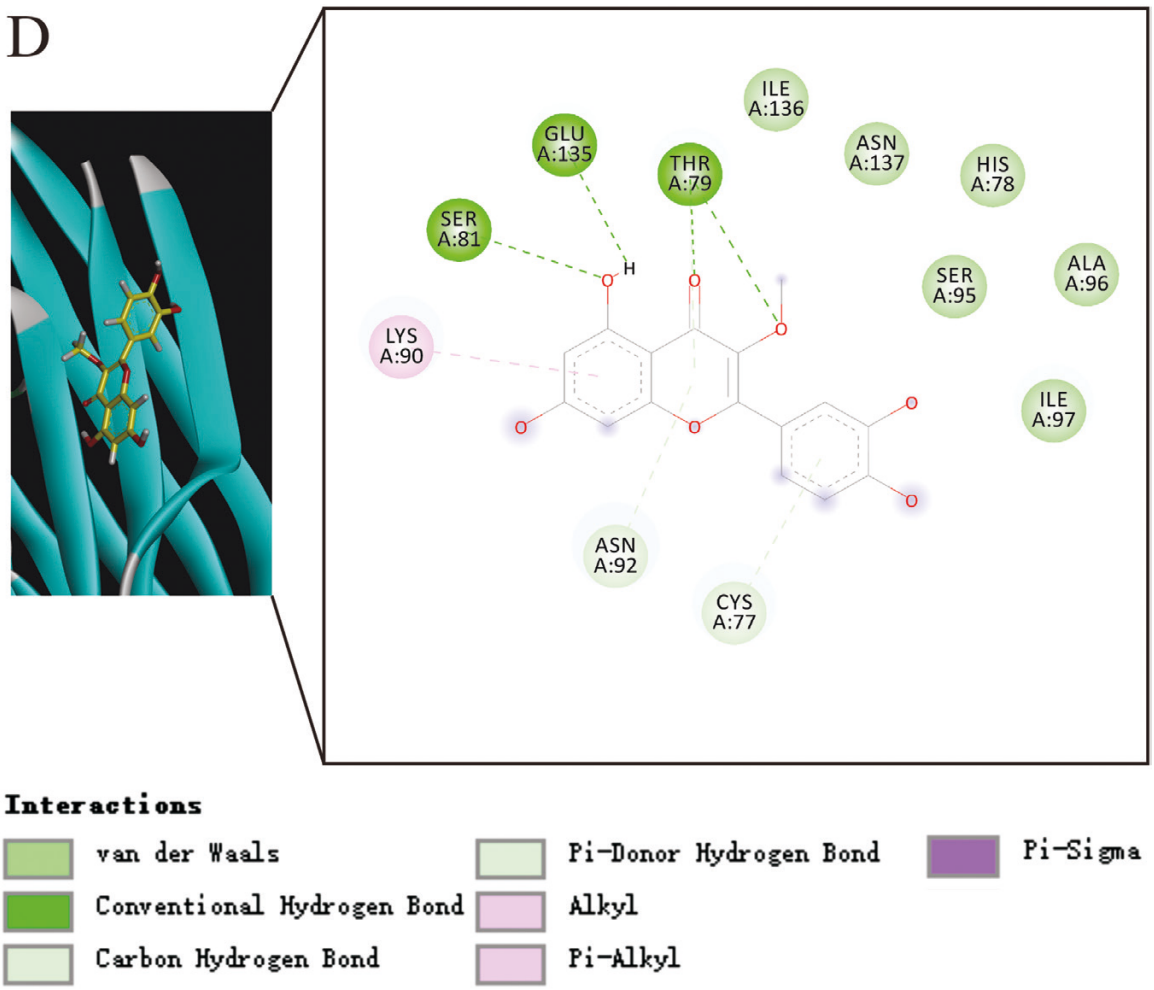


Figure 5. Continued

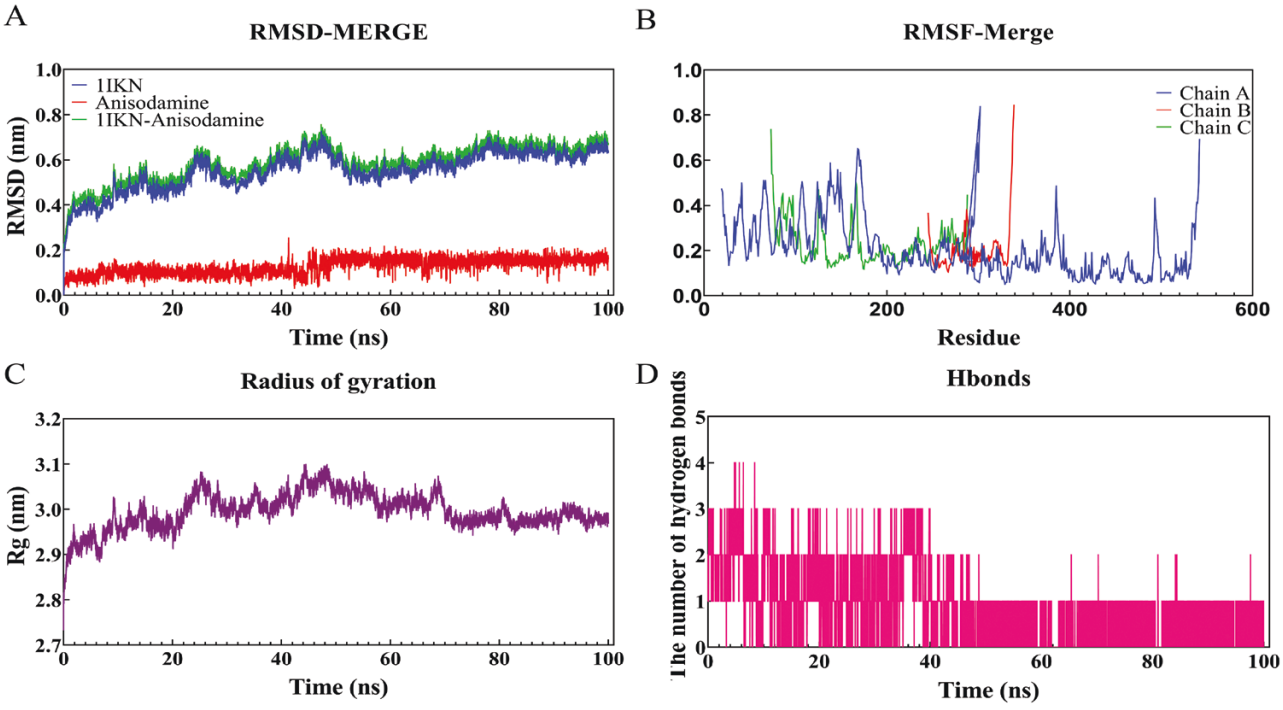


Figure 6. Molecular dynamics simulation of the 1IKN-anisodamine complex. (A) RMSD curve of anisodamine (red line), 1IKN (blue line), and 1IKN-Anisodamine complex (green line). (B) RMSF curve of 1IKN. (C) Rg curve of 1IKN. (D) Hydrogen bonds of the 1IKN-anisodamine complex.

Downloaded from https://academic.oup.com/jpp/article/76/10/1362/7716259 by guest on 25 July 2025

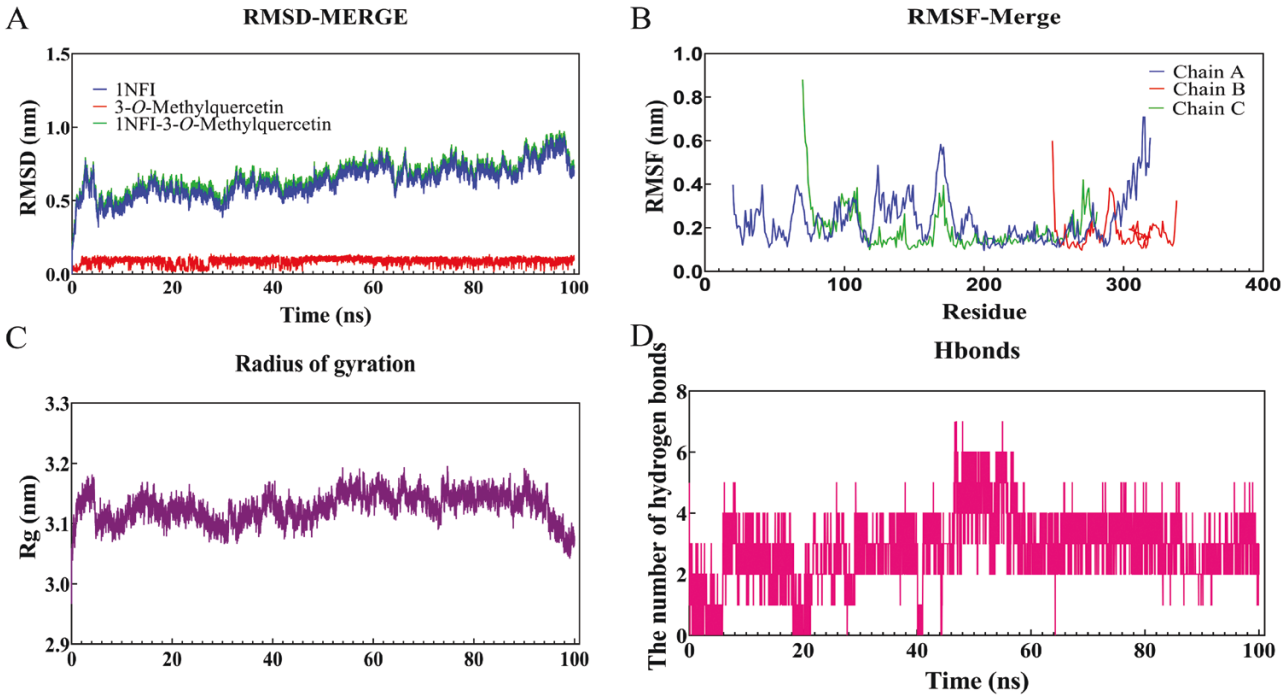


Figure 7. Molecular dynamics simulation of the 1NFI-3-*O*-methylquercetin complex. (A) RMSD curve of 3-*O*-methylquercetin (red line), 1NFI (blue line), and 1NFI-3-*O*-methylquercetin complex (green line). (B) RMSF curve of 1NFI. (C) Rg curve of 1NFI. (D) Hydrogen bonds of the 1NFI-3-*O*-methylquercetin complex.

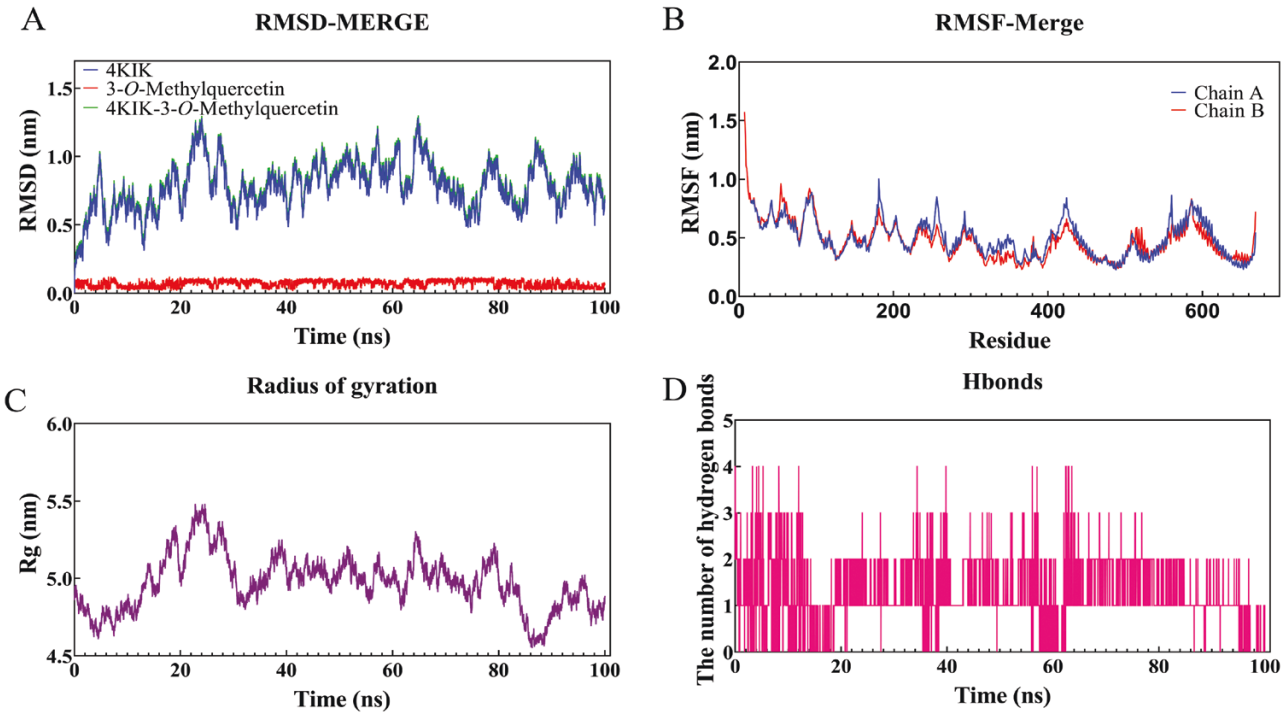


Figure 8. Molecular dynamics simulation of the 4KIK-3-*O*-methylquercetin complex. (A) RMSD curve of 3-*O*-methylquercetin (red line), 4KIK (blue line), and 4KIK-3-*O*-methylquercetin complex (green line). (B) RMSF curve of 4KIK. (C) Rg curve of 4KIK. (D) Hydrogen bonds of the 4KIK-3-*O*-methylquercetin complex.

HSS ameliorated pathological alterations in the lungs of asthmatic mice

To assess the pathological alterations in the lung tissue, H&E staining was done. Comparing the OVA-induced asthma group to the control group, there was a significantly higher level of inflammatory cell infiltration surrounding the bronchi or arteries ($P < 0.01$) (Fig. 11A and B). At the same time, there were obvious compensatory emphysema and local hemorrhage. These alternations were markedly attenuated by the treatment with the concentration of HSS

Downloaded from https://academic.oup.com/jpp/article/76/10/1362/7716259 by guest on 25 July 2025

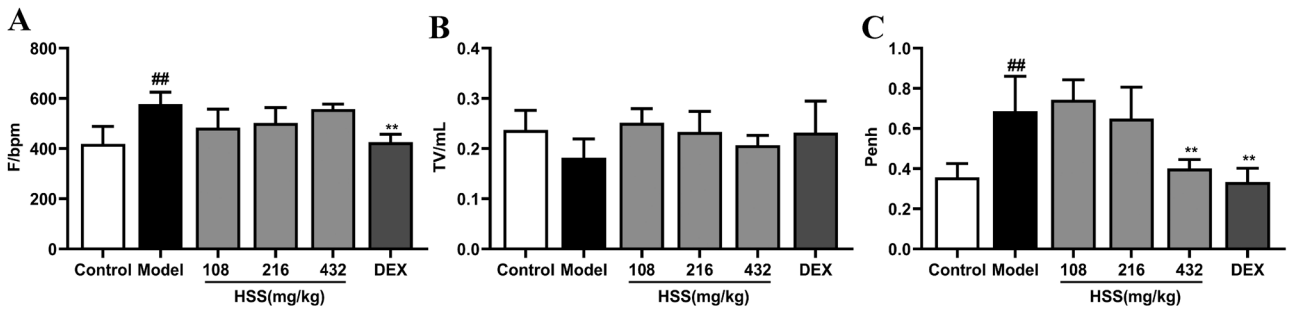


Figure 9. Effects of HSS on lung functions in mice. (A) Evaluation of F in asthmatic mice. (B) Evaluation of TV in asthmatic mice. (C) Evaluation of Phen in asthmatic mice. Data are expressed as the mean ± SD (n = 6), $^{\#\#}P < 0.01$, vs. the control group; $^{**}P < 0.01$ vs. the model group.

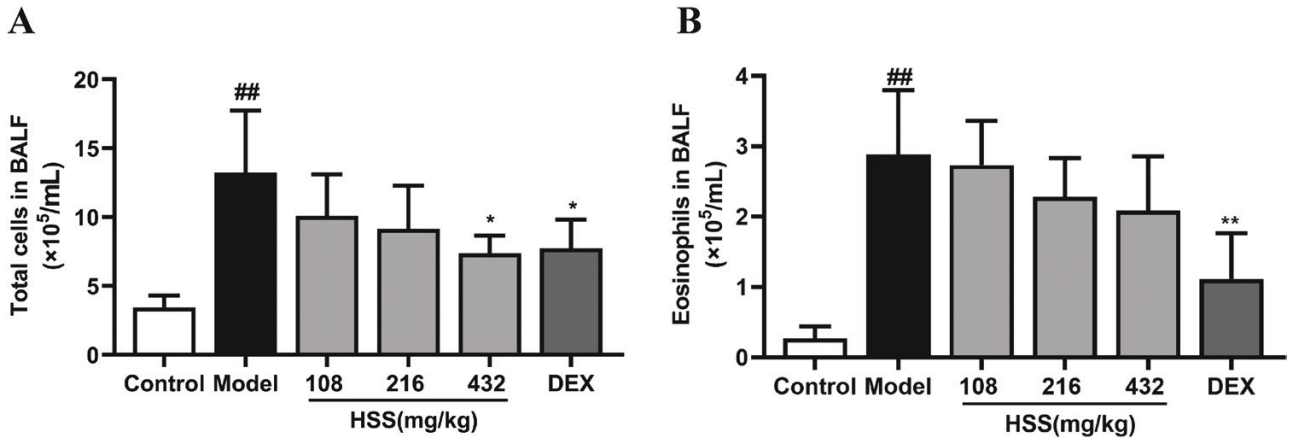


Figure 10. Effects of HSS on inflammatory cell recruitment in BALF detected by cell counting. (A) Total leukocyte numbers in BALF. (B) Eosinophil numbers in BALF. Data are expressed as the mean ± SD (n = 6), $^{\#\#}P < 0.01$, vs. the control group; $^{*}P < 0.05$, and $^{**}P < 0.01$ vs. the model group.

(216 mg/kg) in contrast to the saline-treated animals ($P < 0.05$) (A and B in Fig. 11).

HSS reduced IgE and inflammatory cytokines production in serum and BALF

IgE is an inflammatory factor that contributes to airway inflammation involved in allergic asthma. ELISA was used to measure the blood levels of IgE and OVA-IgE. The results showed a significant elevation in IgE ($P < 0.01$) (Fig. 12A) and OVA-specific IgE production ($P < 0.01$) (Fig. 5B) in the asthmatic mice as opposed to those in the control mice. HSS (432 mg/kg) substantially reduced the secretion of IgE ($P < 0.05$) (Fig. 12A), and significantly reduced the OVA-specific IgE ($P < 0.01$) (Fig. 12B). IL-13, released by Th2 lymphocytes, is associated with the development of many metaplastic diseases. As shown in Fig. 12C, it was revealed that the levels of IL-13 in BALF of the OVA-induced asthmatic mice were substantially elevated in comparison to those of normal mice ($P < 0.01$). However, the addition of HSS inhibited the level of associated cytokines. Notably, the increase IL-13 level in BALF was obviously inhibited in the HSS treatment groups (216 mg/kg) compared to the OVA-induced groups ($P < 0.05$) (Fig. 12D). HSS (432 mg/kg) drastically induced the secretion of TNF-α in the serum contrary to the model group ($P < 0.05$) (Fig. 12E), while TNF-α in BALF was not significantly reduced by treatment with HSS ($P > 0.05$) (Fig. 12F).

HSS suppressed the degree of gene expression associated with inflammation

The amounts of mRNA for IL-4, IL-5, and IL-13 in the Th2 gene family by qRT-PCR were examined. After OVA challenge, increased expression levels of Th2 genes were observed in the OVA-induced mice in contrast to the normal mice. Whereas, the HSS administration (216 mg/kg) dramatically decreased the mRNA levels of IL-4 and IL-13 ($P < 0.05$) (Fig. 13A and C). Nevertheless, compared to the above two genes, the mRNA level of IL-5 in OVA-induced mice was not considerably lowered by HSS therapy ($P > 0.05$) (Fig. 13B).

HSS-treated OVA-induced allergic asthma through NF-κB signaling pathway

Previous reports have suggested that the NF-κB signaling pathway assists with the maintenance of the inflammatory responses in asthma [39]. Furthermore, our results revealed HSS could treat asthma via NF-κB signaling pathway by network pharmacological analysis. In order to validate the result, the expression of NF-κB p65 and phosphorylated protein were evaluated by western blot. To confirm the role of HSS in NF-κB nuclear translocation, immunofluorescence staining for NF-κB p65 was performed.

As shown in Fig. 14A, it was observed that NF-κB p65 was more widespread in the cytoplasm and almost not expressed in the nucleus as observed among the control group. However, in the case of the model group caused by

Downloaded from https://academic.oup.com/jpp/article/76/10/1362/7716259 by guest on 25 July 2025

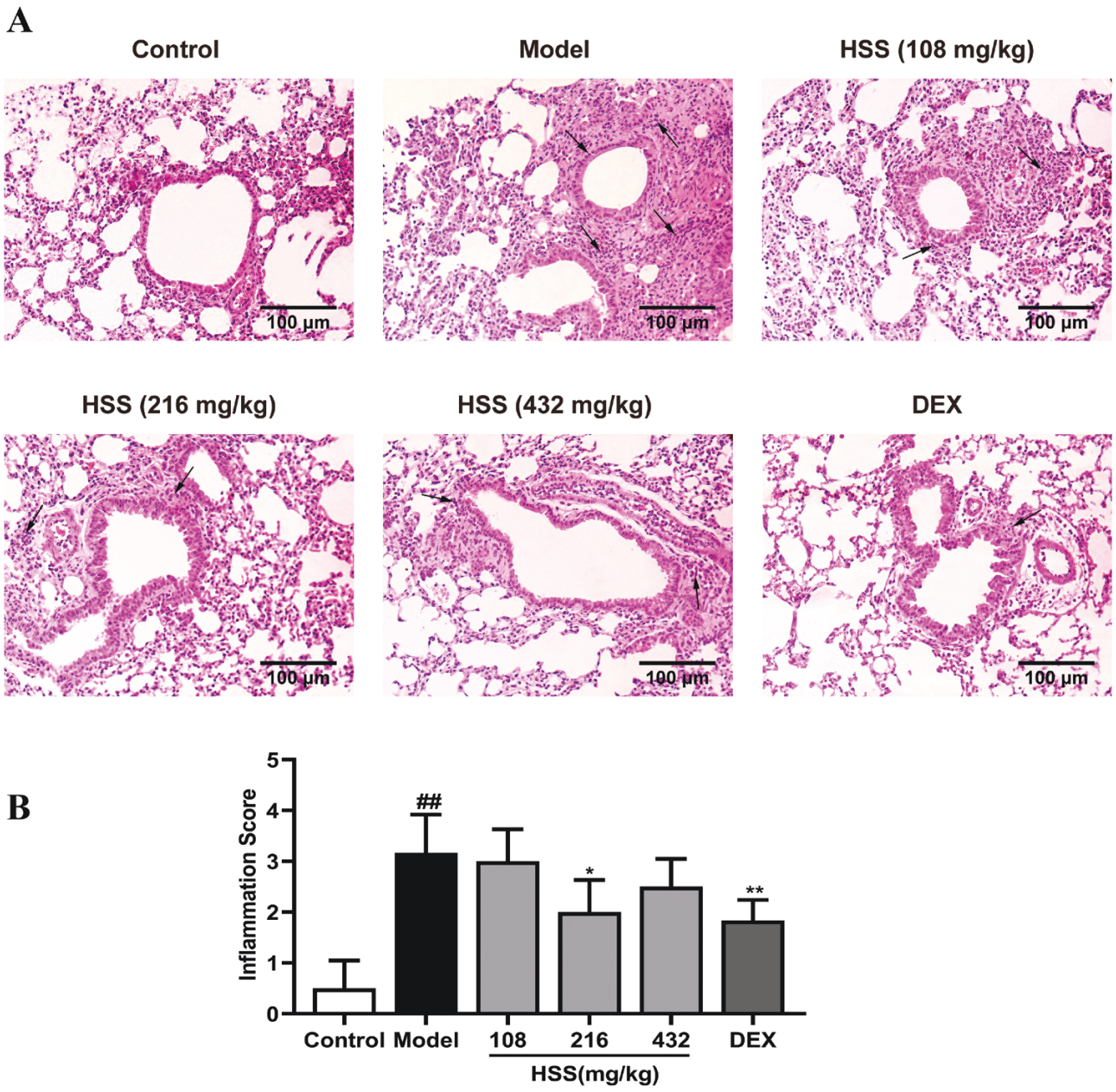


Figure 11. Histopathological analysis of pulmonary sections in the mice. (A) Representative images of H&E staining lung sections. Black arrows indicated infiltrated inflammatory cells (×200); (B) inflammation score of pulmonary sections. Data are expressed as the mean ± SD ($n = 6$), ##$P < 0.01$ vs. the control group; *$P < 0.05$, and **$P < 0.01$ vs. the model group.

OVA, there is an increased nuclear distribution of NF-κB p65. The p65 protein was more expressed in the cytoplasm and less in the nucleus with increasing concentrations of HSS. Therefore, HSS may impede the nuclear translocation of NF-κB p65.

Western blot experiment results suggested the degree of NF-κB p65 phosphorylation was highly expressed within the OVA-induced mice. However, the marked elevation was substantially down-regulated by HSS treatment of 432 mg/kg ($P < 0.05$) (Fig. 14C). Thus, HSS may prevent the inflammation of the airways through suppression of the NF-κB pathway. Mechanistically, HSS could ameliorate allergic inflammation through suppression of NF-κB signaling pathway.

Discussions

Previous research has reported that the anti-asthmatic effects of HSS were due to the suppression of IL-4 and IL-5 production [17]. Unfortunately, the mechanisms of HSS on inflammation are yet unclear. In this research, the potential mechanisms of HSS against asthma were predicted by network pharmacology analysis. The result revealed that NF-κB may be potential target of HSS against inflammation of asthma. Based on the result, an OVA-induced allergic asthma mice model was established and the effects of HSS on NF-κB pathway in allergic asthma were verified. However, the binding energies of hyoscyamine, anisodamine and 3-*O*-methylquercetin with NFKBIA, RELA, IKBKB, and TNF were all less than −5kcal/

Downloaded from https://academic.oup.com/jpp/article/76/10/1362/7716259 by guest on 25 July 2025

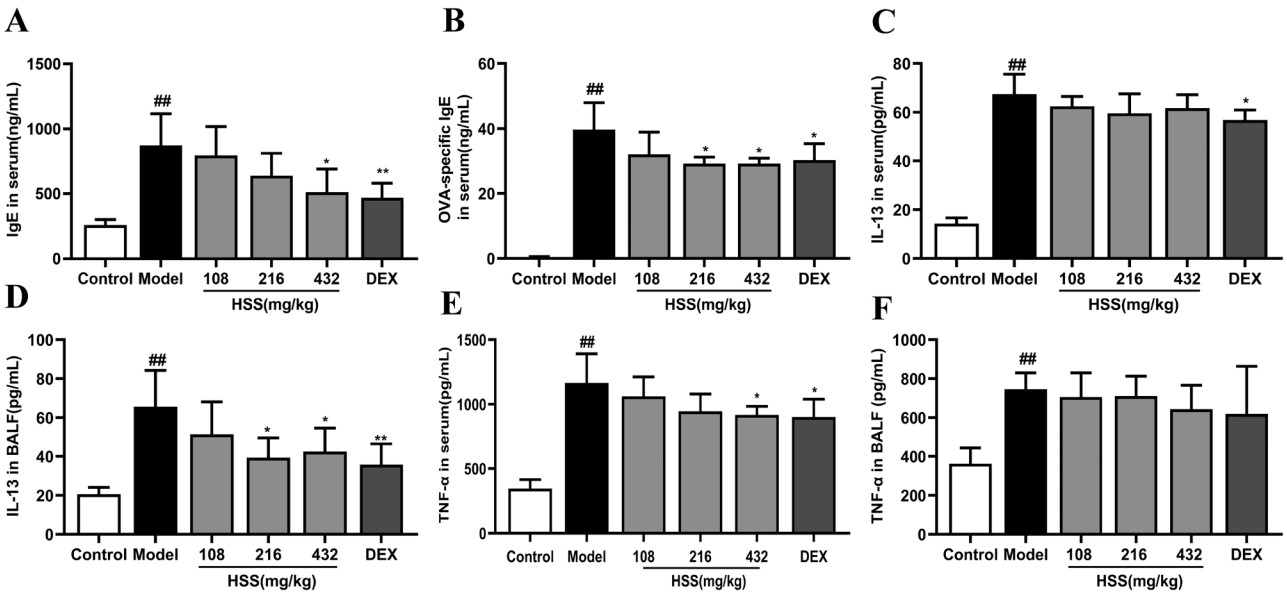


Figure 12. Effects of HSS on IgE and inflammatory cytokine levels in serum and BALF measured by ELISA. (A, B) The levels of IgE and OVA-specific IgE in serum. (C, D) The levels of IL-13 in serum and BALF. (E, F) The levels of TNF-α in serum and BALF. Data are expressed as the mean ± SD (n = 6), ##P < 0.01 vs. the control group; *P < 0.05, and **P < 0.01 vs. the model group.

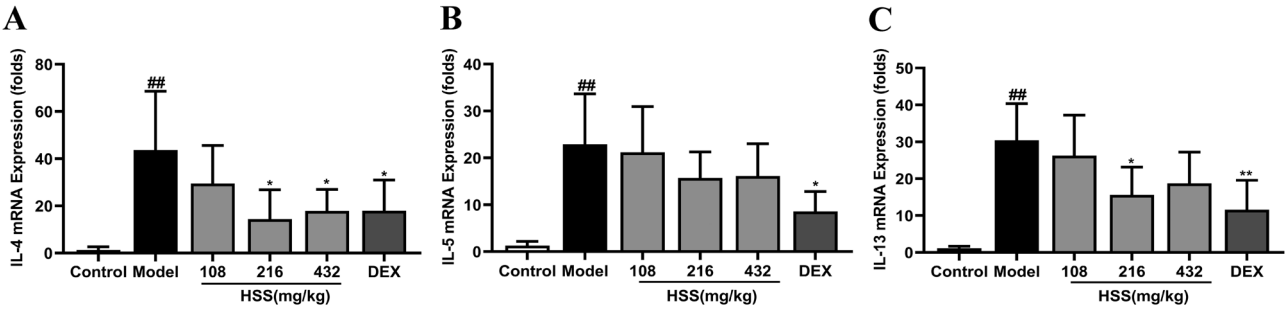


Figure 13. Effects of HSS on the levels of inflammatory cytokines in the lung tissues performed by qRT-PCR. (A) The mRNA levels of IL-4. (B) The mRNA levels of IL-5. (C) The mRNA levels of IL-13. Data are expressed as the mean ± SD (n = 6), ##P < 0.01 vs. the control group; *P < 0.05, **P < 0.01 vs. the model group.

mol, indicating that they all have good interactions and are the active components of HSS. Then, only the four complexes with the highest binding energy were selected for visual analysis, and the analysis was not sufficient, which was the defect and deficiency of this paper.

Inflammation and related pathological changes involved in asthma result in impaired lung function, including increased pulmonary resistance. In the current research, the findings indicated that there was a tendency of HSS to improve the lung functions of OVA-induced mice. It is generally believed that allergic asthma is a kind of chronic inflammatory illness, with characteristics like as increased eosinophil infiltration and mucus production [40]. Eosinophils are a critical effector associated with pathological airway inflammatory changes in OVA-induced mice [41]. Interestingly, HSS induced a remarkable reduction in the elevated leukocytes in BALF, while reducing the number of eosinophils in different doses. In addition, the histopathological analysis showed that HSS dramatically inhibited inflammatory infiltration in the asthma model induced by OVA.

The pathogenesis of asthma has been systematically shown to be complex, with dysfunction of the immune system recognized as a critical component within the underlying pathologies [42]. Relevant research has reported the important role played by an imbalance towards a Th2 response in the pathogenesis of asthma, resulting in the presence of IgE and the production of Th2 lymphocyte cytokines [43]. IL-4 is required for B cell isotype flipping, which results in the production of IgE [44]. IgE is regarded as a key mediator involved in the type I hypersensitivity reaction, combining with the receptors of mast cells to cause allergen-induced asthma [45]. IL-13 is involved in recruiting eosinophils to the airways and producing IgE, which is required for the development of inflammation [46]. IL-5 is also critical for eosinophil activation and survival [47]. Additionally, TNF-α, which plays a role in the start of the inflammatory reaction in asthma, is a cytokine released by mononuclear macrophages. Studies have shown that high levels of TNF-α may contribute to inflammatory cell adhesion to vessels involved in airway remodeling [48].

Here, the study showed that HSS induced reduction in serum IgE and OVA-specific IgE levels, whereas serum and BALF levels of IL-13 and TNF-α were similarly reduced. Furthermore, as reported in a previous study, the expression

Downloaded from https://academic.oup.com/jpp/article/76/10/1362/7716259 by guest on 25 July 2025

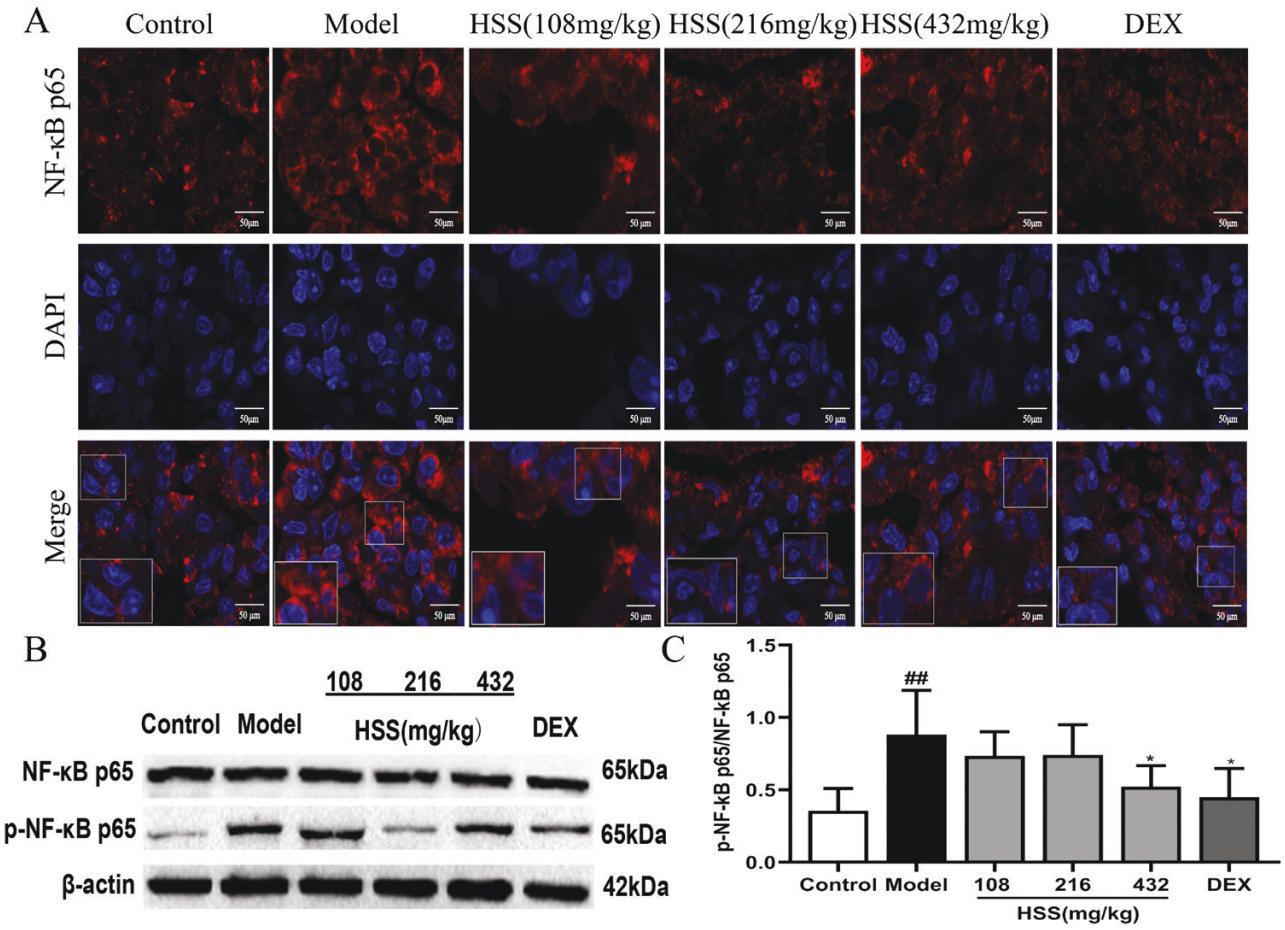


Figure 14. Effects of HSS on NF-κB signaling pathway in OVA-induced mice. (A) Representative immunofluorescence images of colocalization of NF-κB p65 (red) and DAPI (blue) in the lungs of OVA-induced mice detected by immunofluorescence (×400). (B and C) The protein level of p-NF-κB p65 and NF-κB p65 were detected by western blot and protein band was analyzed by Image J. The results were expressed as the ratio of p-NF-κB p65 relative to NF-κB p65. Data are expressed as the mean ± SD (n = 6), $^{\#\#}P < 0.01$ vs. the control group; $^{*}P < 0.05$ vs. the model group.

of IL-4, IL-5, and IL-13 genes was noticeably increased in asthma patients [49]. Hence, we also detected the above Th2 cytokine mRNA by qRT-PCR in the asthmatic mice as well as in the HSS-treated mice. The outcome indicated that HSS induced the suppression of Th2 cytokine mRNA expression in the OVA-induced asthma mice. Besides, increased IgE and IL-13 were observed in the asthma mice, but decreased in the mice with HSS treatment. Concomitantly, increased IgE levels in asthma may be correlated with the increase in IL-13. Moreover, as previous research has shown, the absence of the IL-5 cytokine may lead to a diminution effect in the eosinophil counts [50]. The results showed that HSS induced a reduction in IL-5 expression as well as the eosinophil numbers, in keeping with the opinions of the above study.

As such, the study hypothesized that HSS may reduce the IgE levels by preventing the regulation of IL-13 and IL-4, and the decrease in the Th2 cytokines could account for the effect of HSS treatment on eosinophil numbers. Overall, a reduction in the levels of IgE and Th2 cytokines may assist in reducing allergic inflammation by ameliorating the Th2 immune response.

The transduction of NF-κB was studied to understand the anti-inflammatory role played by HSS. NF-κB becomes activated when it separates from the inhibitory protein IκBα, which is degraded by IκBα. Therefore, NF-κB p65 phosphorylation is characterized by airway inflammation in asthma [51]. Additionally, NF-B is crucial in the inflammatory response by controlling genes downstream, for instance, the cytokines IL-4, IL-5, and IL-13. In that case, this research found that the phosphorylation level of NF-κB p65 was elevated in the OVA-challenged mice compared to control mice, and the administration of HSS attenuated the increased phosphorylation level induced by OVA. Consistently, these results demonstrated that exposure to OVA could lead to NF-κB activation in asthmatic mice, which is consistent with previous studies [52-54] but HSS could ameliorate airway inflammation in OVA-induced asthmatic mice by suppressing the NF-κB signal transduction. Therefore, we hypothesized that the mechanism of the anti-inflammatory effect of HSS may be connected to the adjustment of NF-κB signaling transduction among the asthmatic mice induced by OVA.

Conclusions

Although there is no effective treatment for asthma, effective management would ideally improve and regulate the condition. In clinical application, HSS has an impact on reducing symptoms for asthma sufferers. In this investigation, through network pharmacological analysis and pharmacological

Downloaded from https://academic.oup.com/jpp/article/76/10/1362/7716259 by guest on 25 July 2025

experiments, the efficacy of HSS in OVA-induced allergic asthma was evaluated and the mechanism of HSS relieving asthma inflammation was revealed. The findings of this investigation indicate that HSS can treat OVA-induced allergic asthma by activation of NF-κB pathway. In addition to laying the groundwork for the later disclosure of the mechanism of action of TCM compounds in the treatment of lung diseases, this study offers a fresh perspective on how HSS treats allergic asthma. This opens the door to further investigation into the mysterious mechanisms by which TCM compounds treat various diseases.

Author contributions

Rui Liu, Yansu Ji, and Xin Jin conceived and designed the experiments. Yanhong Xu and Yujie Wu performed research. Wang Xiaoyu and Zhou Miaomiao analyzed the data. Wang Xiaoyu wrote the manuscript. Rui Liu and Jihong Feng directed the research and revised the paper. All authors read and approved the final manuscript.

Conflict of interest

None declared.

Funding

This research was financially supported by Scientific and technological projects entrusted by enterprises and institutions [HX2021-22]. Innovation Research Project of Chinese People's Armed Police Force [ZZKY20222419], and Program for Science and Technology of Logistics University of Chinese People's Armed Police Force [WHJ202301], the Young Qihuang Scholar of the "Tens of millions" talent project of the people republic of China.

Consent for publication

This manuscript was published with the approval of all authors, and there was no conflict of interest in the submission.

Data availability

All data that supports the findings of this study are available from the corresponding author on reasonable request.

References

1. Mortimer K, Reddel HK, Pitrez PM *et al*. Asthma management in low and middle income countries: case for change. *Eur Respir J* 2022;**60**:2103179. https://doi.org/10.1183/13993003.03179-2021
2. Tong S, Yin Y, Bao Y. Climatotherapy for asthma: research progress and prospect. *Environ Res* 2022;**214**:113988. https://doi.org/10.1016/j.envres.2022.113988
3. Caramori G, Nucera F, Mumby S *et al*. Corticosteroid resistance in asthma: cellular and molecular mechanisms. *Mol Aspects Med* 2022;**85**:100969. https://doi.org/10.1016/j.mam.2021.100969
4. Matera MG, Page C, Rinaldi B. β2-Adrenoceptor signalling bias in asthma and COPD and the potential impact on the comorbidities associated with these diseases. *Curr Opin Pharmacol* 2018;**40**:142–6. https://doi.org/10.1016/j.coph.2018.04.012
5. Yamauchi K, Ogasawara M. The role of histamine in the pathophysiology of asthma and the clinical efficacy of antihistamines in asthma therapy. *Int J Mol Sci* 2019;**20**:1733. https://doi.org/10.3390/ijms20071733
6. Schatz M, Rosenwasser L. The allergic asthma phenotype. *J Allergy Clin Immunol Pract* 2014;**2**:645–8; quiz 649. https://doi.org/10.1016/j.jaip.2014.09.004
7. Huang YC, Weng CM, Lee MJ *et al*. Endotypes of severe allergic asthma patients who clinically benefit from anti-IgE therapy. *Clin Exp Allergy* 2019;**49**:44–53. https://doi.org/10.1111/cea.13248
8. Gallagher A, Edwards M, Nair P *et al*. Anti-interleukin-13 and anti-interleukin-4 agents versus placebo, anti-interleukin-5 or anti-immunoglobulin-E agents, for people with asthma. *Cochrane Database Syst Rev* 2021;**10**:CD012929. https://doi.org/10.1002/14651858.CD012929.pub2
9. Alharbi KS, Fuloria NK, Fuloria S *et al*. Nuclear factor-kappa B and its role in inflammatory lung disease. *Chem Biol Interact* 2021;**345**:109568. https://doi.org/10.1016/j.cbi.2021.109568
10. Zhou BW, Liu HM, Jia XH. The role and mechanisms of traditional Chinese medicine for airway inflammation and remodeling in asthma: overview and progress. *Front Pharmacol* 2022;**13**:917256. https://doi.org/10.3389/fphar.2022.917256
11. Man S, Cui N, Liu X *et al*. Component analysis and antiasthmatic effects of Huashanshen dripping pill. *Med Chem Res* 2020;**29**:75–82. https://doi.org/10.1007/s00044-019-02460-z
12. Zhou M, Ma X, Sun J *et al*. Active fragments-guided drug discovery and design of selective tropane alkaloids using ultra-high performance liquid chromatography-quadrupole time-of-flight tandem mass spectrometry coupled with virtual calculation and biological evaluation. *Anal Bioanal Chem* 2017;**409**:1145–57. https://doi.org/10.1007/s00216-016-0043-6
13. Lou Y, Nie G, Li Z. HPLC determination of scopoletin in *Physochlainae Radix*. *Chin J Pharm Anal* 2011;**31**:1137–39.
14. Lv Z, Yao G, Ge M *et al*. Qualitative identification and quantitative comparison of *Physochlainae Radix* from different regions based on chemometric methods. *J Sep Sci* 2023;**46**:e2300475. https://doi.org/10.1002/jssc.202300475
15. Zhao S, Chou G, Wang Z. Chemical constituents from roots and rhizomes of *Physochlaina infundibularis*. *Chin Tradit Herb Drugs* 2013;**44**:938–41.
16. Tan JY, Li JL, Li P *et al*. Two new amides from *Physochlainae Radix*. *Chem Biodivers* 2023;**20**:e202300556. https://doi.org/10.1002/cbdv.202300556
17. Xu ZP, Wang H, Hou LN *et al*. Modulatory effect of anisodamine on airway hyper-reactivity and eosinophilic inflammation in a murine model of allergic asthma. *Int Immunopharmacol* 2011;**11**:260–5. https://doi.org/10.1016/j.intimp.2010.12.001
18. Bui TT, Kwon DA, Choi DW *et al*. *Rosae multiflorae* fructus extract and its four active components alleviate ovalbumin-induced allergic inflammatory responses via regulation of Th1/Th2 imbalance in BALB/c rhinitis mice. *Phytomedicine* 2019;**55**:238–48. https://doi.org/10.1016/j.phymed.2018.06.044
19. Vasconcelos JF, Teixeira MM, Barbosa-Filho JM *et al*. Effects of umbelliferone in a murine model of allergic airway inflammation. *Eur J Pharmacol* 2009;**609**:126–31. https://doi.org/10.1016/j.ejphar.2009.03.027
20. Ko WC, Shih CM, Chen MC *et al*. Suppressive effects of 3-O-methylquercetin on ovalbumin-induced airway hyperresponsiveness. *Planta Med* 2004;**70**:1123–7. https://doi.org/10.1055/s-2004-835838
21. Liu B, Deng X, Jiang Q *et al*. Scoparone alleviates inflammation, apoptosis and fibrosis of non-alcoholic steatohepatitis by suppressing the TLR4/NF-κB signaling pathway in mice. *Int Immunopharmacol* 2019;**75**:105797. https://doi.org/10.1016/j.intimp.2019.105797
22. Kearley J, Buckland KF, Mathie SA *et al*. Resolution of allergic inflammation and airway hyperreactivity is dependent upon disruption of the T1/ST2-IL-33 pathway. *Am J Respir Crit Care Med* 2009;**179**:772–81. https://doi.org/10.1164/rccm.200805-666OC
23. Cheng C, Zhu R, Liu M *et al*. Kunxian capsule alleviates renal damage by inhibiting the JAK1/STAT1 pathway in lupus nephritis.

Downloaded from https://academic.oup.com/jpp/article/76/10/1362/7716259 by guest on 25 July 2025

J Ethnopharmacol 2023;**310**:116349. https://doi.org/10.1016/j.jep.2023.116349
24. Ru J, Li P, Wang J *et al*. TCMSP: a database of systems pharmacology for drug discovery from herbal medicines. *J Cheminform* 2014;**6**:13. https://doi.org/10.1186/1758-2946-6-13
25. Daina A, Michielin O, Zoete V. SwissADME. a free web tool to evaluate pharmacokinetics, drug-likeness and medicinal chemistry friendliness of small molecules. *Sci Rep* 2017;**7**:42717. https://doi.org/10.1038/srep42717
26. Daina A, Michielin O, Zoete V. Swiss target prediction: updated data and new features for efficient prediction of protein targets of small molecules. *Nucleic Acids Res* 2019;**47**:W357–64. https://doi.org/10.1093/nar/gkz382
27. Stelzer G, Rosen N, Plaschkes I *et al*. The GeneCards Suite: from gene data mining to disease genome sequence analyses. *Curr Protoc Bioinformatics* 2016;**54**:1.30.1–1.30.33. https://doi.org/10.1002/cpbi.5
28. Piñero J, Saüch J, Sanz F *et al*. The DisGeNET cytoscape app: exploring and visualizing disease genomics data. *Comput Struct Biotechnol J* 2021;**19**:2960–7. https://doi.org/10.1016/j.csbj.2021.05.015
29. Amberger JS, Bocchini CA, Schiettecatte F *et al*. OMIM.org: Online Mendelian Inheritance in Man (OMIM®), an online catalog of human genes and genetic disorders. *Nucleic Acids Res* 2015;**43**:D789–98. https://doi.org/10.1093/nar/gku1205
30. Szklarczyk D, Morris JH, Cook H *et al*. The STRING database in 2017: quality-controlled protein-protein association networks, made broadly accessible. *Nucleic Acids Res* 2017;**45**:D362–8. https://doi.org/10.1093/nar/gkw937
31. Zhou Y, Zhou B, Pache L *et al*. Metascape provides a biologist-oriented resource for the analysis of systems-level datasets. *Nat Commun* 2019;**10**:1523. https://doi.org/10.1038/s41467-019-09234-6
32. Abraham MJ, Murtola T, Schulz R *et al*. GROMACS: high performance molecular simulations through multi-level parallelism from laptops to supercomputers. *SoftwareX* 2015;**1-2**:19–25. https://doi.org/10.1016/j.softx.2015.06.001
33. Van Der Spoel D, Lindahl E, Hess B *et al*. GROMACS: fast, flexible, and free. *J Comput Chem* 2005;**26**:1701–18. https://doi.org/10.1002/jcc.20291
34. Prada-Dacasa P, Urpi A, Sánchez-Benito L *et al*. Measuring breathing patterns in mice using whole-body plethysmography. *Bio Protoc* 2020;**10**:e3741. https://doi.org/10.21769/BioProtoc.3741
35. Wang J, Gao S, Zhang J *et al*. Interleukin-22 attenuates allergic airway inflammation in ovalbumin-induced asthma mouse model. *BMC Pulm Med* 2021;**21**:385. https://doi.org/10.1186/s12890-021-01698-x
36. Sulimov VB, Kutov DC, Sulimov AV. Advances in docking. *Curr Med Chem* 2019;**26**:7555–80. https://doi.org/10.2174/0929867325666180904115000
37. Kohl M, Wiese S, Warscheid B. Cytoscape: software for visualization and analysis of biological networks. *Methods Mol Biol* 2011;**696**:291–303. https://doi.org/10.1007/978-1-60761-987-1_18
38. Neuhaus-Steinmetz U, Glaab T, Daser A *et al*. Sequential development of airway hyperresponsiveness and acute airway obstruction in a mouse model of allergic inflammation. *Int Arch Allergy Immunol* 2000;**121**:57–67. https://doi.org/10.1159/000024298
39. Lomask M. Further exploration of the Penh parameter. *Exp Toxicol Pathol* 2006;**57**:13–20. https://doi.org/10.1016/j.etp.2006.02.014
40. Lin CC. Noninvasive method to measure airway obstruction in nonanesthetized allergen-sensitized and challenged mice. *Respiration* 2001;**68**:178–85. https://doi.org/10.1159/000050489
41. Fahy JV. Type 2 inflammation in asthma—present in most, absent in many. *Nat Rev Immunol* 2015;**15**:57–65. https://doi.org/10.1038/nri3786
42. Maspero J, Adir Y, Al-Ahmad M *et al*. Type 2 inflammation in asthma and other airway diseases. *ERJ Open Res* 2022;**8**:00576–2021. https://doi.org/10.1183/23120541.00576-2021
43. Khalaf K, Paoletti G, Puggioni F *et al*. Asthma from immune pathogenesis to precision medicine. *Semin Immunol* 2019;**46**:101294. https://doi.org/10.1016/j.smim.2019.101294
44. Lambrecht BN, Hammad H, Fahy JV. The cytokines of asthma. *Immunity* 2019;**50**:975–91. https://doi.org/10.1016/j.immuni.2019.03.018
45. Wade-Vallance AK, Allen CDC. Intrinsic and extrinsic regulation of IgE B cell responses. *Curr Opin Immunol* 2021;**72**:221–9. https://doi.org/10.1016/j.coi.2021.06.005
46. Humbert M, Bousquet J, Bachert C *et al*. IgE-mediated multimorbidities in allergic asthma and the potential for omalizumab therapy. *J Allergy Clin Immunol Pract* 2019;**7**:1418–29. https://doi.org/10.1016/j.jaip.2019.02.030
47. Iwaszko M, Biały S, Bogunia-Kubik K. Significance of interleukin (IL)-4 and IL-13 in inflammatory arthritis. *Cells* 2021;**10**:3000. https://doi.org/10.3390/cells10113000
48. Farne HA, Wilson A, Milan S *et al*. Anti-IL-5 therapies for asthma. *Cochrane Database Syst Rev* 2022;**7**:CD010834. https://doi.org/10.1002/14651858.CD010834.pub4
49. Ricciardolo FLM, Folkerts G, Folino A *et al*. Bradykinin in asthma: modulation of airway inflammation and remodelling. *Eur J Pharmacol* 2018;**827**:181–8. https://doi.org/10.1016/j.ejphar.2018.03.017
50. Humbert M, Durham SR, Ying S *et al*. IL-4 and IL-5 mRNA and protein in bronchial biopsies from patients with atopic and nonatopic asthma: evidence against "intrinsic" asthma being a distinct immunopathologic entity. *Am J Respir Crit Care Med* 1996;**154**:1497–504. https://doi.org/10.1164/ajrccm.154.5.8912771
51. Yu H, Lin L, Zhang Z *et al*. Targeting NF-κB pathway for the therapy of diseases: mechanism and clinical study. *Signal Transduct Target Ther* 2020;**5**:209. https://doi.org/10.1038/s41392-020-00312-6
52. Bai D, Sun T, Lu F *et al*. Eupatilin suppresses OVA-induced asthma by inhibiting NF-κB and MAPK and activating Nrf2 signaling pathways in mice. *Int J Mol Sci* 2022;**23**:1582. https://doi.org/10.3390/ijms23031582
53. Piao CH, Song CH, Lee EJ *et al*. Saikosaponin A ameliorates nasal inflammation by suppressing IL-6/ROR-γt/STAT3/IL-17/NF-κB pathway in OVA-induced allergic rhinitis. *Chem Biol Interact* 2020;**315**:108874. https://doi.org/10.1016/j.cbi.2019.108874
54. Zhang Q, Wang L, Chen B *et al*. Propofol inhibits NF-κB activation to ameliorate airway inflammation in ovalbumin (OVA)-induced allergic asthma mice. *Int Immunopharmacol* 2017;**51**:158–64. https://doi.org/10.1016/j.intimp.2017.08.015

Downloaded from https://academic.oup.com/jpp/article/76/10/1362/7716259 by guest on 25 July 2025